αSMA-Expressing Perivascular Cells Represent Dental Pulp Progenitors In Vivo

Vidović Zdrilić, Ivana; Banerjee, A.; Fatahi, R.; Matthews, B.G.; Dyment, N.A.; Kalajzić, I.; Mina, M.

Source / Izvornik: **Journal of Dental Research, 2016, 96, 323 - 330**

Journal article, Published version
Rad u časopisu, Objavljena verzija rada (izdavačev PDF)

https://doi.org/10.1177/0022034516678208

Permanent link / Trajna poveznica: https://urn.nsk.hr/urn:nbn:hr:184:908187

Journal of Dental Research
2017, Vol. 96(3) 323–330

DOI: 10.1177/0022034516678208
journals.sagepub.com/home/jdr

αSMA-Expressing Perivascular Cells Represent Dental Pulp Progenitors In Vivo

I. Vidovic[1], A. Banerjee[1], R. Fatahi[2], B.G. Matthews[2], N.A. Dyment[2], I. Kalajzic[2], and M. Mina[1]

Abstract

The goal of this study was to examine the contribution of perivascular cells to odontoblasts during the development, growth, and repair of dentin using mouse molars as a model. We used an inducible, Cre-loxP in vivo fate-mapping approach to examine the contributions of the descendants of cells expressing the αSMA-CreERT2 transgene to the odontoblast lineage. In vivo lineage-tracing experiments in molars showed the contribution of αSMA-tdTomato$^+$ cells to a small number of newly formed odontoblasts during primary dentinogenesis. Using an experimental pulp exposure model in molars to induce reparative dentinogenesis, we demonstrate the contribution of αSMA-tdTomato$^+$ cells to cells secreting reparative dentin. Our results demonstrate that αSMA-tdTomato$^+$ cells differentiated into Col2.3-GFP$^+$ cells composed of both *Dspp*$^+$ odontoblasts and *Bsp*$^+$ osteoblasts. Our findings identify a population of mesenchymal progenitor cells capable of giving rise to a second generation of odontoblasts during reparative dentinogenesis. This population also makes a small contribution to odontoblasts during primary dentinogenesis.

Keywords: odontoblasts, pulp biology, dentinogenesis, reparative dentin, stem cells, dentin sialophosphoprotein

Introduction

The dentin-pulp complex has regenerative potential, leading to the formation of tertiary dentin. Mild stimuli lead to reactionary dentinogenesis, during which pre-existing odontoblasts upregulate their secretory activity (Sloan and Smith 2007; Sloan and Waddington 2009). However, trauma of greater intensity that causes death of the pre-existing odontoblasts leads to reparative dentinogenesis involving the recruitment of progenitor cells to the site of injury, proliferation, and differentiation into a second generation of odontoblasts or "odontoblast-like cells" (Sloan and Smith 2007; Sloan and Waddington 2009). These odontoblast-like cells synthesize reparative dentin immediately below the site of damage to preserve pulp vitality (Sloan and Smith 2007; Sloan and Waddington 2009). Available evidence suggests that the pulp contains several niches of potential progenitors/stem cells involved in reparative dentinogenesis (Sloan and Smith 2007; Sloan and Waddington 2009).

Mesenchymal stem cells (MSCs) have been identified from various organs based on limited criteria including their adherent (nonhematopoietic), clonogenic potential, expression of various surface markers, and in vitro trilineage differentiation (Bianco and Robey 2015). The in vivo identity of MSCs and their supporting niche in many organs remains elusive and is being studied using various techniques including label-retaining and lineage-tracing analyses. Many of these studies indicated that MSCs in many organs reside in a perivascular niche and that MSCs originate from pericytes, which are perivascular cells that wrap around endothelial cells in capillaries and microvessels (Crisan et al. 2008; Crisan et al. 2009; Crisan et al. 2011; Gökçinar-Yagci et al. 2015). Recent studies suggested differences between MSCs in pericapillaries and perivenous areas (Corselli et al. 2012). Perivascular cells can be identified/isolated based on the expression of several markers including CD146, chondroitin sulfate proteoglycan 4 (NG2), platelet-derived growth factor receptor-beta (PDGF-Rβ), and alpha-smooth muscle actin (αSMA) (Crisan et al. 2008; Crisan et al. 2009; Crisan et al. 2011).

MSC populations have also been described in teeth and their supporting structures and are collectively referred to as dental MSCs (Ledesma-Martínez et al. 2016; Sharpe 2016). Among these, MSCs of the dental pulp share many in vivo and in vitro similarities with skeletal stem cells in bone marrow. The dental pulp, similar to bone marrow, is a highly vascularized, innervated soft tissue, and several studies have shown that MSCs in the dental pulp and bone marrow are capable of differentiating into mineral-producing cells, namely, odontoblasts and osteoblasts, respectively (Ledesma-Martínez et al. 2016; Sharpe 2016).

[1]Department of Craniofacial Sciences, School of Dental Medicine, University of Connecticut Health Center, Farmington, CT, USA
[2]Department of Reconstructive Sciences, School of Dental Medicine, University of Connecticut Health Center, Farmington, CT, USA

A supplemental appendix to this article is available online.

Corresponding Author:
M. Mina, Department of Craniofacial Sciences, School of Dental Medicine, University of Connecticut Health Center, 263 Farmington Avenue, Farmington, CT 06030, USA.
Email: Mina@nso1.uchc.edu

In recent years, there have also been significant advances in our understanding of dental MSCs involved in the growth and repair of odontoblasts in continuously growing rodent incisors. These studies have indicated that the dental pulp of the incisor contains several populations of MSCs, which include slow-cycling mesenchymal cells expressing Thy1 located between the lingual and labial cervical loops, peripheral nerve–associated glial cells, periarterial Gli1-expressing cells located in the neural-vascular bundles at the proximal end of the incisor, and NG2-expressing pericytes (Feng et al. 2011; Kaukua et al. 2014; Zhao et al. 2014). A recent study has also shown the contribution of pericyte-derived cells to the odontoblast-like cells in "restorative dentin," which is the mineralizing tissue at the tips of incisors (Pang et al. 2016).

The goal of the present study was to gain insight into the role of perivascular cells expressing αSMACre-tdTomato in primary and reparative dentinogenesis and in the differentiation of odontoblast-like cells using cell lineage–tracing experiments in developing mice molars that are not continuously erupting and are more similar to human dentition.

Materials and Methods

Animal Models

αSMA-GFP, αSMACreERT2/Ai9, and Col2.3-GFP mice have been previously described (Braut et al. 2003; Kalajzic et al. 2008; Balic et al. 2010; Grcevic et al. 2012). For in vivo lineage-tracing experiments, αSMACreERT2/Ai9 mice (cross between αSMACreERT2 with Ai9 Cre reporter mice; Jackson Laboratory) and αSMACreERT2/Ai9;Col2.3-GFP mice (cross between αSMACreERT2/Ai9 with Col2.3-GFP mice; Roguljic et al. 2013) were used. Animal protocols were approved by the Institutional Animal Care Committee. In lineage-tracing studies, neonatal mice were injected intraperitoneally with corn oil (vehicle [VH]) or tamoxifen (TM; 75 μg/g body weight) at P4 and P5 and sacrificed 2 (P7), 9 (P14), and 16 (P21) d after the TM injection. The untreated, VH-injected αSMACreERT2 mice and αSMACreERT2$^-$/Ai9 TM-treated mice were examined as controls for spontaneous Cre activation in pulp tissue in vivo.

Flow Cytometric Analysis

Freshly isolated dental pulp tissue from P7 molars of αSMA-GFP transgenic mice was prepared for fluorescence-activated cell sorting (FACS) analysis by mild trypsin/ethylenediaminetetraacetic acid (EDTA) digestion as described previously (Balic et al. 2010). Data were processed using CellQuest software (BD Biosciences). Nontransgenic littermates were used as controls. For analysis of CD45, CD31, CD90, and Sca1, cells were incubated with antibodies.

Experimental Pulp Exposure/Injury

Four-wk-old transgenic mice were injected with TM or VH twice with a 24-h interval; 2 d later, mice were anesthetized with an intraperitoneal injection of ketamine (87 mg/kg) and xylazine (13 mg/kg) and prepared for experimental pulp exposure on the maxillary first molars. A class I cavity was prepared with a round carbide bur (diameter, 0.30 mm) on the occlusal surface of the maxillary molars (Frozoni et al. 2012). Pulp exposure was subsequently created mechanically using an endodontic hand file (tip diameter, 0.08–0.10 mm). The exposed pulp was capped using mineral trioxide aggregate mixed with sterile water following the manufacturer's recommendations. Mineral trioxide aggregate was placed in contact with the pulp using an endodontic spreader tip and condensed gently. Subsequently, the cavity was sealed with light-cured composite resin associated with a 1-step self-etching adhesive system. Animals were sacrificed by intracardiac perfusion with 4% paraformaldehyde in phosphate-buffered saline (PBS) at the indicated time points (Frozoni et al. 2012).

Histological Analysis

After perfusion, the maxilla was dissected, fixed in 4% paraformaldehyde overnight at 4°C, and decalcified in 14% EDTA for 3 to 7 d. Decalcified tissue was placed in 30% sucrose solution overnight and embedded in Shandon Cryomatrix (Thermo Fisher Scientific). Seven-micrometer sections were obtained using a Leica cryostat and mounted using the CryoJane tape transfer system (Leica Biosystems). Sections were examined and imaged using a Zeiss Z1 microscope with filter cubes optimized for green fluorescent protein (GFP), tdTomato, and DAPI variants. Adjacent sections were processed for hematoxylin and eosin staining and analyzed by light microscopy.

For analysis of the fate of αSMA-tdTomato$^+$ cells, all sections through the site of injury and repair and sections of control uninjured teeth (12–20 sections per tooth) were evaluated. For evaluation of the injury and repair, 3 to 6 animals were analyzed per time point. The areas of red-labeled cells in the pulp chambers were calculated using ImageJ software (National Institutes of Health).

Immunohistochemical Analysis

Cryosections were incubated in the Power Block (BioGenex) for 20 min at 20°C. After washing with PBS, the sections were incubated with anti-mouse CD31 primary antibody (1:200, BD Biosciences) at 4°C overnight. Sections were washed and exposed to secondary antibody (donkey anti-goat immunoglobulin G (IgG) labeled with Alexa Fluor 488, 1:500, Thermo Fisher Scientific, or donkey anti-goat IgG labeled with Texas Red, 1:500, Santa Cruz Biotechnology) for 1 h at 20°C.

Fluorochrome Labeling of Mineralizing Surfaces

The dynamic process of mineral apposition in newly formed reparative dentin was examined after weekly intraperitoneal injections of fluorescent dyes dissolved in 2% $NaHCO_3$ (pH 7.4). These injections started 1 wk after pulp exposure and included calcein green (CG; 6 mg/kg), demeclocycline (DC; 60 mg/kg),

calcein blue (CB; 60 mg/kg), and once again CG (Sigma-Aldrich). Animals were sacrificed by intracardiac perfusion and processed for histology 1 d after the injection of the last dye.

RNAscope In Situ Hybridization

In situ hybridization was conducted on frozen sections using the RNAscope 2.5 HD Reagent Kit–BROWN (Advanced Cell Diagnostics) for *Dspp* and *Bsp* according to the manufacturer's instructions.

Results

Characterization of αSMA Expression during Mouse Molar Development

Previous immunohistochemical analyses showed high levels of αSMA expression in the dental follicle of rat molars (Hosoya et al. 2006) and αSMA-GFP expression in periodontal tissue of mouse molars (San Miguel et al. 2010). In this study, using αSMA-GFP transgenic mice (Kalajzic et al. 2008; San Miguel et al. 2010; Roguljic et al. 2013), we first examined the expression of this transgene in the dental pulp and odontoblasts in developing molars and incisors at various stages of development (P7, P14, and P21, 4 and 6 wk old). At all stages, αSMA-GFP$^+$ cells were detected in bone marrow in the alveolar bone and dental pulp of molars and incisors (Fig. 1 and Appendix Fig. 1). The expression of αSMA-GFP was not detected in odontoblasts, ameloblasts, cementoblasts, or osteoblasts (Fig. 1A–H and Appendix Fig. 1A–L). The strong expression of αSMA-GFP was detected in the dental follicle of molars at P7 (Fig. 1A, B) and dental follicles surrounding the cervical loops of incisors (Appendix Fig. 1A, B, G, H). In the molars, a few αSMA-GFP$^+$ cells were detected in the stellate reticulum (Fig. 1B). αSMA-GFP was detected in periodontal ligament fibers after root formation (P21 and older animals) (Fig. 1E).

Immunohistochemical staining with CD31 antibody that identifies endothelial cells showed the close proximity of αSMA-GFP$^+$ cells to CD31$^+$ cells in various locations including the dental pulp (Fig. 1I, J). Analysis of the freshly isolated dental pulp from P7 αSMA-GFP transgenic animals by flow cytometry showed that αSMA-GFP$^+$ cells constituted a small fraction of pulp cells (<5% of the total cell number) and did not express hematopoietic (CD45) or endothelial (CD31) markers (Appendix Fig. 2). Approximately 22% of αSMA-GFP$^+$ cells expressed stem cell marker Sca1, and about half expressed CD90 (Appendix Fig. 2).

αSMA Perivascular Cells Contribute to Odontoblasts during Growth and Development

Since αSMA-GFP is not expressed by odontoblasts, to gain a better understanding of the roles of αSMA$^+$ perivascular cells during dentinogenesis, we used Cre-mediated genetic lineage tracing with αSMA-CreERT2 transgenic mice (Grcevic et al. 2012). In these animals, CreERT2 recombinase is targeted by

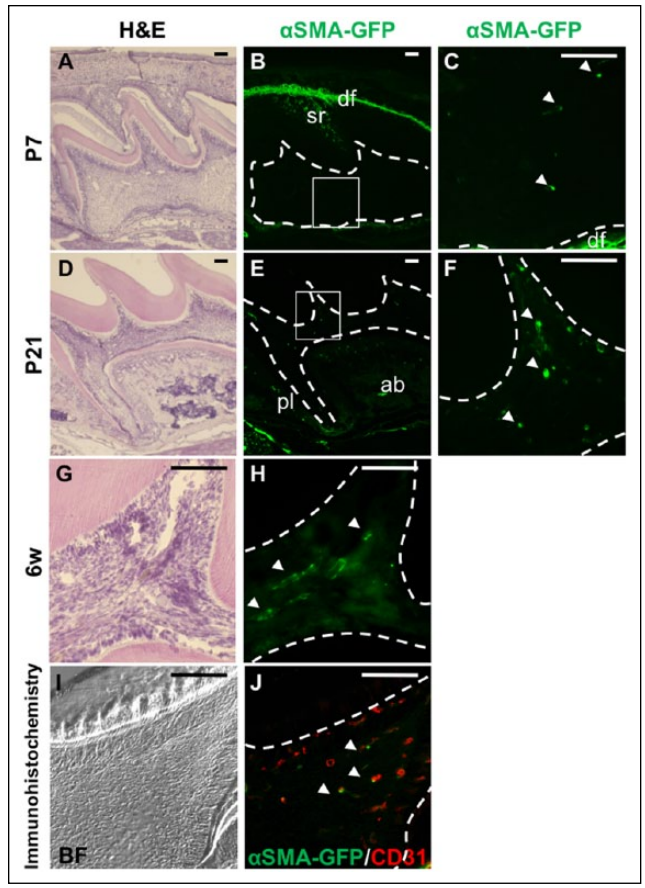

Figure 1. Expression of the αSMA-GFP transgene in developing molars in vivo. Representative hematoxylin and eosin–stained and epifluorescent images of adjacent sagittal sections of maxillary first molars from αSMA-GFP transgenic mice at P7 (**A–C**), P21 (**D–F**), and 6 wk old (**G, H**). C is a higher magnification of the boxed area in B, and F is a higher magnification of the boxed area in E. αSMA-GFP is expressed in the dental follicle (df) extending to the stellate reticulum (sr) (B). αSMA-GFP is also expressed in the dental pulp (C, E, F, H), and αSMA-GFP is detected in periodontal ligament (pl) fibers at P21. Bright field (**I**) and epifluorescent (**J**) images of a sagittal section of a maxillary first molar at P7 from αSMA-GFP transgenic mice. The section was stained with CD31 antibody. Note the close association of αSMA-GFP$^+$ cells (green) with CD31$^+$ endothelial cells (red). In all images, the pulp chambers are denoted by dashed lines, and αSMA-GFP$^+$ cells in the dental pulp are indicated by arrowheads. Scale bars =100 μm. ab, alveolar bone.

the regulatory elements of αSMA (the same elements driving GFP expression in αSMA-GFP mice). The administration of TM at specific time points (pulse) activates CreERT2 in cells expressing the transgene. Crossing these mice with Cre-dependent Ai9 reporter mice (Rosa26-tdTomato) enabled the visualization of αSMA$^+$ cells and their progenies expressing the tdTomato fluorescent protein (referred to as αSMA-tdTomato$^+$ cells) over a long period of time.

Pups were injected at P4 and P5 with TM to label cells. The fate of αSMA-tdTomato$^+$ cells was followed at 2 (at P7, during crown morphogenesis), 9 (at P14, time of initiation of root formation that occurs after completion of crown formation), and 16 (P21, during root elongation) d after the injection (Fig. 2A). The specificity of Cre activation was examined in VH-injected

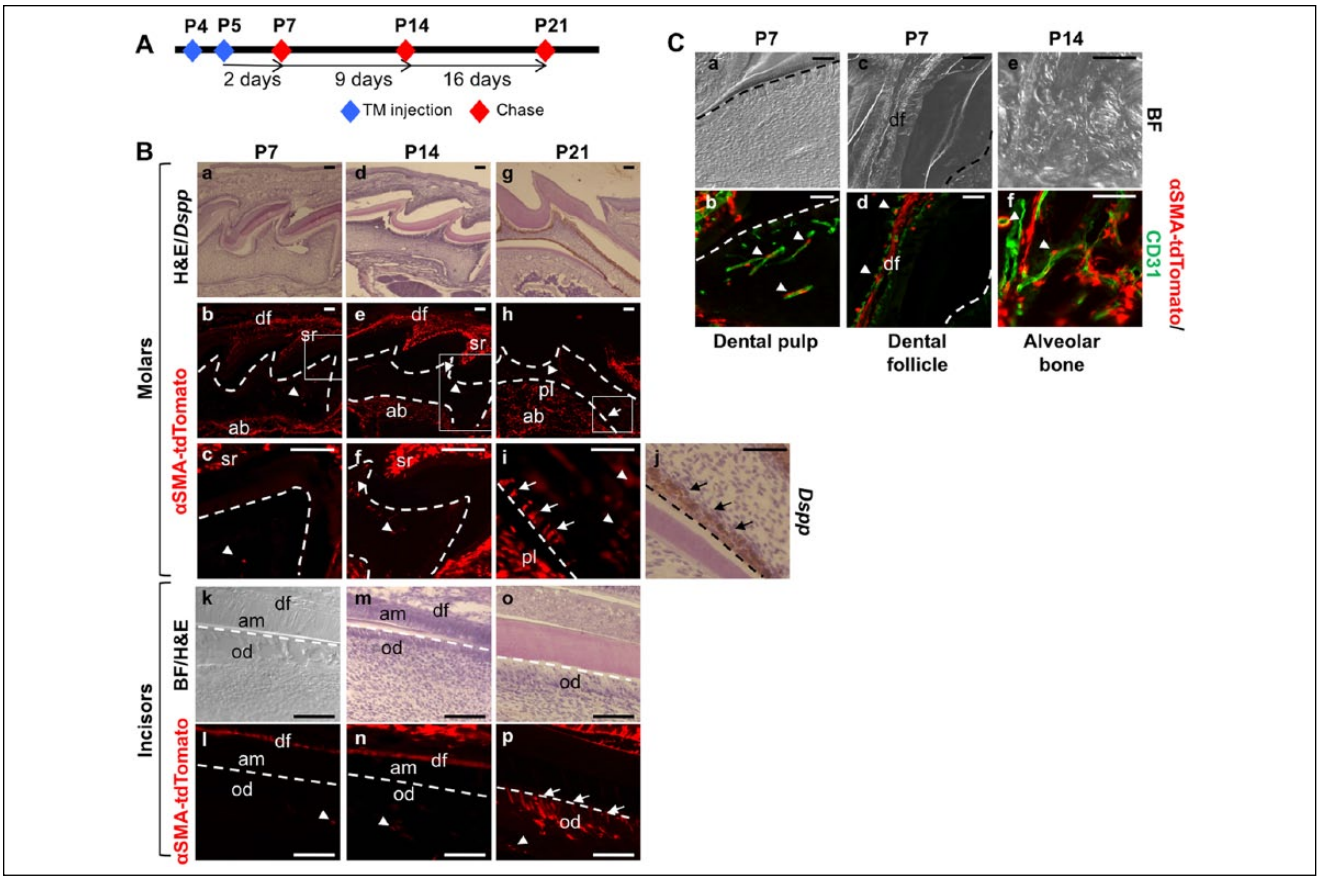

Figure 2. αSMA-tdTomato$^+$ cells give rise to odontoblasts in developing molars and incisors. (**A**) Scheme of lineage-tracing experiments in which αSMACreERT2/Ai9 transgenic mice were injected with tamoxifen (TM) at P4 and P5 and chased at indicated time points. (**B**) Representative hematoxylin and eosin (H&E)–stained (a, d, g) and epifluorescent (b, e, h) images of adjacent sagittal sections of maxillary first molars at 2 d (P7, a–c), 9 d (P14, d–f), and 16 d (P21, g–j) after the TM injection. The section shown in g was processed for RNAscope in situ hybridization for *Dspp* and then stained with H&E. c, f, and i are a higher magnification of the boxed areas in b, e, and h. In the molars, αSMA-tdTomato$^+$ cells are detected in the dental follicle (df) extending to the stellate reticulum (sr) and a few cells in the pulp (arrowheads) at P7 (b and c) and P14 (e and f). At P21, αSMA-tdTomato$^+$ cells are detected in marrow spaces in the alveolar bone (ab), periodontal ligament (pl), and dental pulp. Note the αSMA-tdTomato$^+$ cells in the newly formed odontoblasts (arrows) in the developing root (h and i). j is a higher magnification of g showing the expression of *Dspp* in odontoblasts in the root expressing αSMA-tdTomato$^+$ cells in the adjacent section shown in i. Representative H&E-stained (k, m, o) and epifluorescent (k, n, p) images of adjacent sagittal sections of mandibular incisors at 2 d (P7, k, l), 9 d (P14, m, n), and 16 d (P21, o, p) after the TM injection. In the incisors at P7, P14, and P21, αSMA-tdTomato$^+$ cells are expressed in the dental pulp. Note the absence of αSMA-tdTomato$^+$ cells in odontoblasts (od) and ameloblasts (am) at P7 and P14 (l and n). Note the αSMA-tdTomato$^+$ cells in newly formed odontoblasts (arrows) at P21 (p). (**C**) Representative images of sections of maxillary molars at P7 (a–d) and the maxillary alveolar bone at P14 (e and f) from αSMACreERT2/Ai9 transgenic mice. All sections were stained with CD31 antibody. Note the close association of αSMA-tdTomato$^+$ (arrowheads) with CD31$^+$ endothelial cells (green) in the dental pulp, dental follicle, and alveolar bone. In all images, the dental pulp is denoted by dashed lines. Scale bars = 100 μm.

animals, which showed the absence of αSMA-tdTomato$^+$ in developing teeth and surrounding tissue at all time points after the injection (Appendix Fig. 3A, B).

Moreover, 2 d after the injection, few αSMA-tdTomato$^+$ cells were detected in the dental pulp, dental follicle, and bone marrow in the alveolar bone (Fig. 2B a–c). In all 3 locations, αSMA-tdTomato$^+$ was expressed in close proximity to CD31$^+$ cells (Fig. 2C a–f). A few αSMA-tdTomato$^+$ cells were also detected in the stellate reticulum. The number of αSMA-tdTomato$^+$ cells in these locations increased after 9 and 16 d after the injection (Fig. 2B b–h). αSMA-tdTomato$^+$ cells were not detected in ameloblasts and odontoblasts 2 and 9 d after the injection (Fig. 2B a–f). However, 16 d after the injection, a few αSMA-tdTomato$^+$ cells were detected in newly formed *Dspp*$^+$ odontoblasts in forming roots (Fig. 2B g–j).

In the incisors, the strong expression of αSMA-tdTomato was detected in dental follicles surrounding the cervical loops (Appendix Fig. 3C b, f, j), in the dental pulp (Appendix Fig. 3C d, h, i), and in bone marrow in the alveolar bone. In odontoblasts, the expression of αSMA-tdTomato was not detected 2 and 9 d after the injection (Fig. 2B k–n). However, at P21, a few αSMA-tdTomato$^+$ cells were detected in odontoblasts located midway between the tip and cervical loop on the labial side of the incisor (Fig. 2B o, p). Taken together, these observations indicate a small contribution of αSMA$^+$ cells to odontoblasts during development and growth.

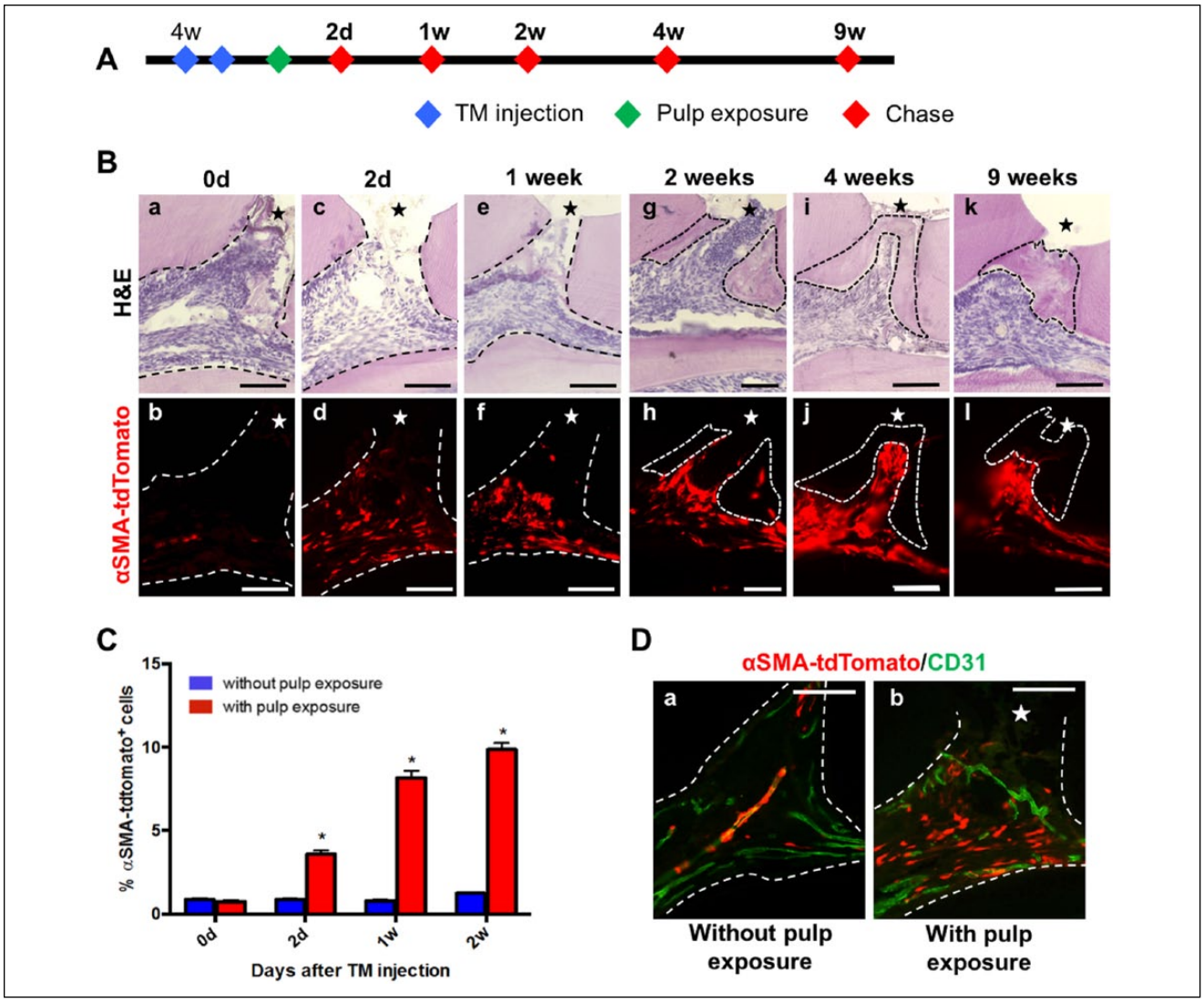

Figure 3. Early and late response of αSMA-tdTomato$^+$ cells to pulp exposure. (**A**) Scheme of lineage-tracing experiments in αSMACreERT2/Ai9 transgenic mice during reparative dentinogenesis. Four-wk-old animals were injected with tamoxifen (TM) twice with a 24-h interval. Pulp exposure was performed 48 h after the second injection, and animals were chased at indicated time points after pulp exposure. (**B**) Representative hematoxylin and eosin–stained and epifluorescent images of adjacent sagittal sections of maxillary first molars with pulp exposure at various time points. In all images, newly formed mineralized tissue (reparative dentin) is denoted by solid lines, the dental pulp by dashed lines, and the site of pulp exposure by an asterisk. Note that αSMA-tdTomato$^+$ cells are in association with (surrounding and lining) forming reparative dentin (h, j, and l). (**C**) Histogram showing the changes in αSMA-tdTomato$^+$ in the pulp of maxillary molars with and without pulp exposure. Note the significant increases in the percentage of αSMA-tdTomato$^+$ cells in the dental pulp after pulp exposure. Results represent the mean ± SEM in at least 3 independent experiments; $P \leq 0.05$ relative to control at each time point in 3 independent experiments. (**D**) Representative epifluorescent images of sections of intact (a) and injured maxillary molars of αSMACreERT2/Ai9 animals 2 d after pulp exposure (b). Sections were stained with CD31 antibody (green). Note the changes in the localization of αSMA-tdTomato$^+$ cells after pulp exposure (b) as compared to intact teeth (a). Scale bars = 100 μm.

Early Response of αSMA-tdTomato$^+$ Cells to Pulp Exposure

To examine the effects of pulp injuries on αSMA-tdTomato$^+$ cells in vivo, we used lineage tracing and experimental pulp exposure to induce reparative dentinogenesis on the maxillary first molars in 4-wk-old αSMACreERT2/Ai9 transgenic mice. In these experiments, animals were first injected with TM (twice with a 24-h interval), followed by experimental pulp exposure. The fate of αSMA-tdTomato$^+$ cells was examined 2 d to 9 wk after pulp exposure (Fig. 3A). The removal of dentin and odontoblasts after experimental pulp exposure was confirmed using Col2.3-GFP transgenic animals (Appendix Fig. 4A). Uninjured and injured first maxillary molars from VH-injected animals and uninjured, contralateral first maxillary molars from the TM-injected animals were used as controls. αSMA-tdTomato$^+$ cells were not detected in the pulp of VH-injected animals (Appendix Fig. 4B–D).

Pulp exposure resulted in the expansion of αSMA-tdTomato$^+$ as early as 2 d after the injury as compared to intact

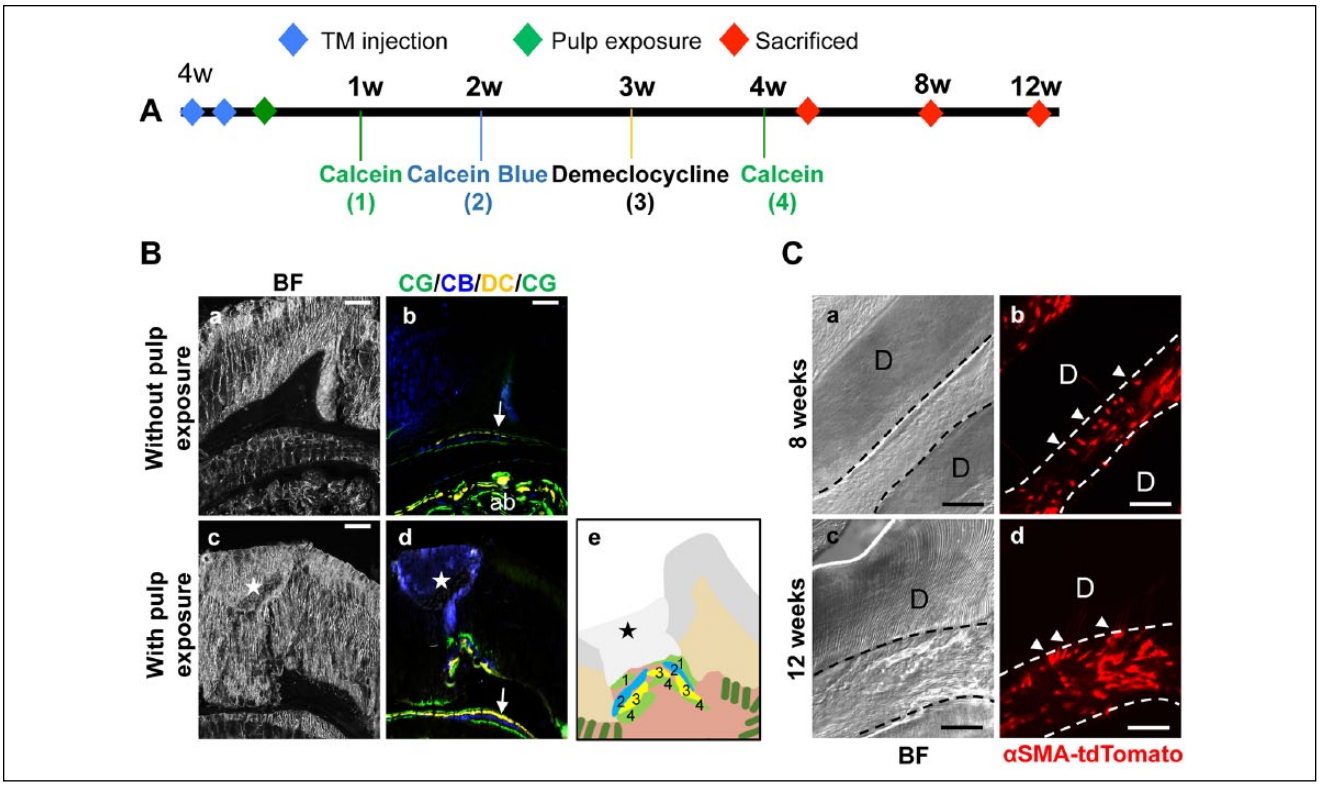

Figure 4. Deposition of new mineralized tissue during secondary and reparative dentinogenesis. (**A**) Scheme of fluorochrome labeling in tamoxifen (TM)-injected αSMACreERT2/Ai9 transgenic mice after pulp exposure. (**B**) Representative bright field (BF) and epifluorescent images of sections of a maxillary molar without (a and b) and with (c and d) pulp exposure. e is a schematic drawing of fluorochrome labeling in d. Numbers in e correspond to fluorochrome labels shown in A. Note the presence of 4 separate lines of fluorochrome labels in the mineralized bridge formed at the site of pulp exposure (asterisk). Also note the deposition of all 4 fluorochrome labels on the floor of the pulp chamber (arrow) and underlying alveolar bone (ab) in intact molars (b). (**C**) Representative bright field and epifluorescent images of sections of the root (a, b) and the floor of the pulp chamber (c, d) of maxillary molars at 8 wk (a and b) and 12 wk (c and d) after the injury. In these images, dashed lines denote the pulp, and αSMA-tdTomato$^+$ odontoblasts are indicated by arrowheads. Note the few αSMA-tdTomato$^+$ odontoblasts in both locations. D, dentin. Scale bars = 100 μm.

teeth (Fig. 3B b, F as compared to Appendix Fig. 4C) with continuous increases in the number of αSMA-tdTomato$^+$ cells (Fig. 3C). The pulp injury resulted in the increased frequency of αSMA-tdTomato$^+$ cells throughout the pulp chamber (Fig. 3B a–i), including areas that are distant from the injury (Appendix Fig. 5). Immunohistochemical analysis showed that unlike in intact teeth, in injured teeth, the majority of αSMA-tdTomato$^+$ cells were not perivascular (close association with CD31$^+$ cells) (Fig. 3D).

A reparative process was initiated at 1 to 2 wk, evident by the formation of a calcified matrix on the dentin walls at the site of exposure (Fig. 3B e–h), containing both reparative (atubular) and reactionary (tubular) dentin. A calcified bridge resembling reparative dentin closing the site of exposure was evident at 3 to 4 wk (Fig. 3B i) and was lined and/or surrounded by numerous αSMA-tdTomato$^+$ cells (Fig. 3B j). Analyses at later time points showed continuous increases in the thickness of the reparative/calcified matrix and the number of αSMA-tdTomato$^+$ cells associated with it, suggestive of their roles in the deposition of reparative dentin (Fig. 3B i–k).

To ensure that reparative dentin at the sites of injury resulted from the deposition of new calcified matrices, we performed fluorochrome mineral labeling at different time points (Fig. 4A, B). A histological examination of molars 4 wk after pulp exposure showed 4 irregular and distinct labeled lines in the calcified bridge/reparative dentin formed at the site of injury (Fig. 4B). Four continuous and well-separated labeled lines were evident in the underlying alveolar bone (Fig. 4B b). These lines and a few αSMA-tdTomato$^+$ cells were also evident at sites undergoing secondary dentinogenesis, including the tips of the pulp horns, floor of the pulp chambers, and roots of both intact and injured molars in TM-injected animals (Fig. 4C and data not shown).

Contribution of αSMA-tdTomato$^+$–Derived Cells to Reparative Dentin after Pulp Exposure

Reparative dentin differs from primary and secondary dentin in that it lacks the tubular structure and is often described as "osteodentin" because it contains both odontoblast- and osteoblast-like cells (Sloan and Smith 2007; Sloan and Waddington 2009). To further examine the differentiated progenies of αSMA-tdTomato$^+$–derived cells giving rise to a calcified bridge/reparative dentin at the site of injury, we crossed αSMACreERT2/Ai9 mice with Col2.3-GFP transgenic mice, shown to be expressed by both odontoblasts and osteoblasts (Braut et al. 2003). Experimental pulp exposure was performed on αSMACreERT2/

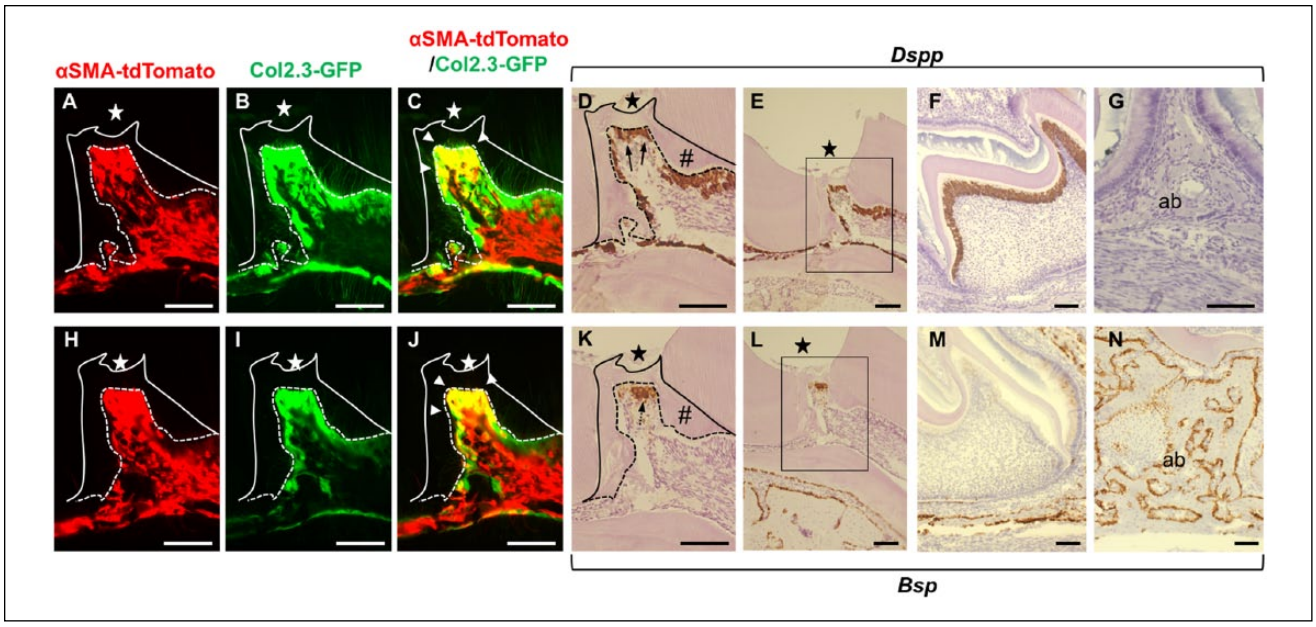

Figure 5. Contribution of αSMA-tdTomato$^+$ cells to odontoblasts, osteoblasts, and reparative dentin. (**A–C**) Representative epifluorescent images of sections of the maxillary molar of an αSMACreERT2/Ai9; Col2.3-GFP animal 4 wk after pulp exposure. **D** and **E** are images from an adjacent section processed for RNAscope in situ hybridization for *Dspp*. A to D are a higher magnification of the boxed area in E showing the site of exposure. Representative images of sections of an intact maxillary arch at P7 showing the expression of *Dspp* in odontoblasts (**F**) and its lack of expression in osteoblasts in the alveolar bone (**G**, ab). (**H–J**) Representative epifluorescent images of another adjacent section of the maxillary molar of the αSMACreERT2/Ai9; Col2.3-GFP animal after pulp exposure. **K** and **L** are images from an adjacent section processed for RNAscope in situ hybridization for *Bsp*. H to K are a higher magnification of the boxed area in L. Representative images of sections of an intact maxillary arch at P7 showing the expression of *Bsp* in osteoblasts of the alveolar bone (**N** ab) and its lack of expression in odontoblasts (**M**). In all these images, the newly formed mineralized tissue is denoted by a solid line. Reactionary tubular dentin is denoted by # in D and K. The dental pulp is denoted by dashed lines and the site of pulp exposure by an asterisk. Note the numerous cells co-expressing αSMA-tdTomato and Col2.3-GFP (yellow, indicated by arrowheads) in cells lining the newly formed mineralized tissue. D and E show the expression of *Dspp* in many cells lining the newly formed mineralized tissue and pre-existing odontoblasts. K and L show the expression of *Bsp* in a subpopulation of cells lining the newly formed mineralized tissue. *Bsp* expression is only detected in cells located below the site of exposure. Note the overlap in the expression of αSMA-tdTomato, Col2.3-GFP, *Dspp*, and *Bsp* in cells underneath the site of exposure. Scale bars = 100 μm.

Ai9; Col2.3-GFP mice after TM injections. A histological examination 4 wk after the injury showed that the newly formed calcified bridge/reparative dentin was lined with both αSMA-tdTomato$^+$ and Col2.3-GFP$^+$ cells. Furthermore, at these locations, there were numerous cells co-expressing both transgenes (Fig. 5A–C, H–J).

The phenotype of the cells co-expressing both transgenes (αSMA-tdTomato$^+$ and 2.3-GFP$^+$) at the sites of injury was further examined by RNAscope in situ hybridization using probes for *Bsp* and *Dspp*, which are markers for differentiated osteoblasts and odontoblasts, respectively (Fig. 5F, G, M, N). The expression of *Dspp* (Fig. 5D–E) and *Bsp* (Fig. 5K–L) was detected in numerous double-labeled cells lining the newly formed calcified bridge/reparative dentin, providing direct evidence for the contribution of αSMA-tdTomato$^+$ cells to both odontoblast- and osteoblast-like cell populations during reparative dentinogenesis. These observations together indicate that perivascular cells expressing αSMA make important contributions to odontoblast-like cells during repair in molars (Fig. 5).

Discussion

Our lineage-tracing studies in developing teeth showed a small contribution of αSMA-tdTomato$^+$ cells to odontoblasts in the forming molar root and the labial sides of the incisor. The absence of αSMA-tdTomato$^+$ cells in the crown of the molar is related to the time of the TM injection at P4/P5. At this time point, morphogenesis of the crown is completed, whereas roots and odontoblasts are not formed yet. Therefore, the labeled cells are detected in a small number of forming odontoblasts in the root.

The small contribution of αSMA-tdTomato$^+$ cells to odontoblasts during primary dentinogenesis may also be related to variable TM Cre efficiency or due to the contribution of additional αSMA$^-$ resident MSCs to odontoblasts during growth. Previous observations in continuously growing incisors showed the partial contribution of different populations of MSCs including Thy1$^+$, peripheral nerve–associated glial cells, and NG2$^+$ pericytes to odontoblasts during growth (Feng et al. 2011; Kaukua et al. 2014; Zhao et al. 2014). On the other hand, the periarterial Gli1$^+$ cells located in the neural-vascular bundles at the proximal end of the incisor contribute to almost 100% of odontoblasts (Zhao et al. 2014). Further lineage-tracing experiments are necessary to examine the contributions of these different populations of MSCs to odontoblasts during growth and secondary dentinogenesis in molars.

Our lineage-tracing studies showed that injuries to the pulp resulting in the destruction of odontoblasts and dentin led to the expansion of αSMA-tdTomato$^+$ in areas in close vicinity as

well as at a distance from the site of injury. These observations suggest that the signaling pathways leading to the activation and differentiation of MSCs in the pulp after an injury are complex. These pathways include the pathways activated by the release of a number of signaling factors sequestered in the dentin matrix and pulp-supportive tissue (Sloan and Smith 2007; Sloan and Waddington 2009; About 2011). However, there is an increasing body of evidence indicating that in addition to their roles in dentinogenesis, odontoblasts function as sensory cells for detecting nociceptive signals, and odontoblast processes act as sensors for detecting various signals (Bleicher 2014; Kawashima and Okiji 2016). These new findings suggest the involvement of various signaling pathways involved in the detection and/or transduction of stimuli, such as thermal, mechanical, and chemical, in the activation of different populations of MSCs including αSMA-tdTomato$^+$ cells.

Following their activation, αSMA-tdTomato$^+$ cells increased in number, left perivascular locations, and were recruited to the site of injury, where they differentiated into odontoblast-like cells expressing *Dspp* and osteoblast-like cells expressing *Bsp*. These results indicated the differentiation of resident αSMA-tdTomato$^+$ cells to both odontoblast- and osteoblast-like cells, indicating their important contribution to reparative dentinogenesis. Lineage tracing in mice incisors showed the contributions of NG2$^+$ pericytes originating from Gli1$^+$ cells and glia-derived MSCs (Feng et al. 2011; Kaukua et al. 2014; Zhao et al. 2014) to odontoblast-like cells during reparative dentinogenesis.

Collectively, our findings identify a population of mesenchymal progenitor cells capable of giving rise to a second generation of odontoblasts during dentin repair. This population also makes a small contribution to odontoblasts during primary and secondary dentinogenesis. These observations should enable us to gain a better understanding of regulatory mechanisms that direct the differentiation of MSCs to odontoblasts and osteoblasts. This information will have an impact on future studies in dentin repair and the modulation of the differentiation of these cells.

Author Contributions

I. Vidovic, contributed to conception, design, data acquisition, analysis, and interpretation, drafted and critically revised the manuscript; A. Banerjee and R. Fatahi, contributed to conception, design, data acquisition, analysis, and interpretation, drafted the manuscript; B.G. Matthews, N.A. Dyment, I. Kalajzic, and M. Mina, contributed to conception, design, data acquisition, analysis, and interpretation, drafted and critically revised the manuscript. All authors gave final approval and agree to be accountable for all aspects of the work.

Acknowledgments

The authors thank all individuals who provided reagents, valuable input, and technical assistance in various aspects of this study, including Drs. David Rowe and Anamaria Balic, Mrs. Barbara Rodgers, and members of the Molecular Core Facility and Flow Cytometry Facility at the University of Connecticut Health Center. This work was supported by grants R01-DE016689 (M.M.), R01-AR055607 (I.K.), and R90-DE022526 from the National Institutes of Health (National Institute of Dental and Craniofacial Research). The authors declare no potential conflicts of interest with respect to the authorship and/or publication of this article.

References

About I. 2011. Dentin regeneration in vitro: the pivotal role of supportive cells. Adv Dent Res. 23(3):320–324.

Balic A, Aguila HL, Caimano MJ, Francone VP, Mina M. 2010. Characterization of stem and progenitor cells in the dental pulp of erupted and unerupted murine molars. Bone. 46(6):1639–1651.

Bianco P, Robey PG. 2015. Skeletal stem cells. Development. 142(6):1023–1027.

Bleicher F. 2014. Odontoblast physiology. Exp Cell Res. 325(2):65–71.

Braut A, Kollar EJ, Mina M. 2003. Analysis of the odontogenic and osteogenic potentials of dental pulp in vivo using a Col1a1-2.3-GFP transgene. Int J Dev Biol. 47(4):281–292.

Corselli M, Chen CW, Sun B, Yap S, Rubin JP, Péault B. 2012. The tunica adventitia of human arteries and veins as a source of mesenchymal stem cells. Stem Cells Dev. 21(8):1299–1308.

Crisan M, Chen CW, Corselli M, Andriolo G, Lazzari L, Péault B. 2009. Perivascular multipotent progenitor cells in human organs. Ann N Y Acad Sci. 1176:118–123.

Crisan M, Corselli M, Chen CW, Péault B. 2011. Multilineage stem cells in the adult: a perivascular legacy? Organogenesis. 7(2):101–104.

Crisan M, Yap S, Casteilla L, Chen CW, Corselli M, Park TS, Andriolo G, Sun B, Zheng B, Zhang L, et al. 2008. A perivascular origin for mesenchymal stem cells in multiple human organs. Cell Stem Cell. 3(3):301–313.

Feng J, Mantesso A, De Bari C, Nishiyama A, Sharpe PT. 2011. Dual origin of mesenchymal stem cells contributing to organ growth and repair. Proc Natl Acad Sci U S A. 108(16):6503–6508.

Frozoni M, Balic A, Sagomonyants K, Zaia AA, Line SR, Mina M. 2012. A feasibility study for the analysis of reparative dentinogenesis in pOBCol3.6GFPtpz transgenic mice. Int Endod J. 45(10):907–914.

Gökçinar-Yagci B, Uçkan-Çetinkaya D, Çelebi-Saltik B. 2015. Pericytes: properties, functions and applications in tissue engineering. Stem Cell Rev. 11(4):549–559.

Grcevic D, Pejda S, Matthews BG, Repic D, Wang L, Li H, Kronenberg MS, Jiang X, Maye P, Adams DJ, et al. 2012. In vivo fate mapping identifies mesenchymal progenitor cells. Stem Cells. 30(2):187–196.

Hosoya A, Nakamura H, Ninomiya T, Yoshiba K, Yoshiba N, Nakaya H, Wakitani S, Yamada H, Kasahara E, Ozawa H. 2006. Immunohistochemical localization of alpha-smooth muscle actin during rat molar tooth development. J Histochem Cytochem. 54(12):1371–1378.

Kalajzic Z, Li H, Wang LP, Jiang X, Lamothe K, Adams DJ, Aguila HL, Rowe DW, Kalajzic I. 2008. Use of an alpha-smooth muscle actin GFP reporter to identify an osteoprogenitor population. Bone. 43(3):501–510.

Kaukua N, Shahidi MK, Konstantinidou C, Dyachuk V, Kaucka M, Furlan A, An Z, Wang L, Hultman I, Ahrlund-Richter L, et al. 2014. Glial origin of mesenchymal stem cells in a tooth model system. Nature. 513(7519):551–554.

Kawashima N, Okiji T. 2016. Odontoblasts: specialized hard-tissue-forming cells in the dentin-pulp complex. Congenit Anom (Kyoto). 56(4):144–153.

Ledesma-Martínez E, Mendoza-Núñez VM, Santiago-Osorio E. 2016. Mesenchymal stem cells derived from dental pulp: a review. Stem Cells Int. 2016:4709572.

Pang YW, Feng J, Daltoe F, Fatscher R, Gentleman E, Gentleman MM, Sharpe PT. 2016. Perivascular stem cells at the tip of mouse incisors regulate tissue regeneration. J Bone Miner Res. 31(3):514–523.

Roguljic H, Matthews BG, Yang W, Cvija H, Mina M, Kalajzic I. 2013. In vivo identification of periodontal progenitor cells. J Dent Res. 92(8):709–715.

San Miguel SM, Fatahi MR, Li H, Igwe JC, Aguila HL, Kalajzic I. 2010. Defining a visual marker of osteoprogenitor cells within the periodontium. J Periodontal Res. 45(1):60–70.

Sharpe PT. 2016. Dental mesenchymal stem cells. Development. 143(13):2273–2280.

Sloan AJ, Smith AJ. 2007. Stem cells and the dental pulp: potential roles in dentine regeneration and repair. Oral Dis. 13(2):151–157.

Sloan AJ, Waddington RJ. 2009. Dental pulp stem cells: what, where, how? Int J Paediatr Dent. 19(1):61–70.

Zhao H, Feng J, Seidel K, Shi S, Klein O, Sharpe P, Chai Y. 2014. Secretion of shh by a neurovascular bundle niche supports mesenchymal stem cell homeostasis in the adult mouse incisor. Cell Stem Cell. 14(2):160–173.